Available online at www.sciencedirect.com

jmr&t Journal of Materials Research and Technology

www.jmrt.com.br

Original Article

Characterization of the oxide scale formed on external surface of HP reformer tubes☆

Rosa Maria Sales da Silveira[a,*], *Mónica P. Arenas*[a,b], *Clara Johanna Pacheco*[b], *Adriana da Cunha Rocha*[a], *Carlos Bruno Eckstein*[c], *Antonio Carlos Bruno*[d], *Gabriela Ribeiro Pereira*[a,b], *Luiz Henrique de Almeida*[a]

[a] *Department of Metallurgical and Materials Engineering – Alberto Luiz Coimbra Institute for Graduate Studies and Engineering Research-Federal University of Rio de Janeiro (COPPE-UFRJ), Rio de Janeiro, RJ, Brazil*

[b] *Laboratory of Nondestructive Testing, Corrosion and Welding (LNDC), Federal University of Rio de Janeiro (UFRJ), Rio de Janeiro, RJ, Brazil*

[c] *Brazilian Petroleum S.A. (PETROBRAS), Rio de Janeiro, RJ, Brazil*

[d] *Department of Physics, Pontifícia Universidade Católica do Rio de Janeiro, Rio de Janeiro, Brazil*

ARTICLE INFO

Article history:
Received 17 November 2017
Accepted 6 August 2018
Available online 28 August 2018

Keywords:
Oxide scale
High temperature oxidation
Modified HP steel
Steam reforming tubes

ABSTRACT

This work presents the characterization of the external oxide scale of a centrifugally cast HP steel tube, modified with Nb and Ti, after 90,000 h of operation in a steam reforming furnace, showing different aging states as a function of the column height and exposure temperature. The objective was to relate the oxide microstructural morphology to its magnetic response for three different microstructural aging states. The morphological and compositional characterization was performed by high resolution scanning electron microscopy, energy dispersive spectrometer and X-ray diffraction. The magnetic response of the external surface was analyzed by magnetic force microscopy and scanning magnetic susceptometer. The results showed the formation of a multilayer oxide scale with different compositions along its thickness. In addition, a microstructural modification was identified in the scale-matrix interface, due to the depletion of chromium. It was also observed that the magnetic response is dependable both on the oxide scale thickness and the chromium carbides depleted zone. Magnetic force microscopy was able to identify the origin of the magnetic response resulted from the steel tube surface.

☆ Paper was part of technical contributions presented in the events part of the ABM Week 2017, October 2nd to 6th, 2017, São Paulo, SP, Brazil.

* *Corresponding author.*
E-mail: rosasilveira@metalmat.ufrj.br (R.M. Silveira).

https://doi.org/10.1016/j.jmrt.2018.08.001

1. Introduction

Steam reformer furnaces are used for large-scale production of hydrogen. These furnaces operate under severe conditions due to the reactions involving hydrocarbons and steam that produce hydrogen and carbon dioxide [1,2]. These reactions take place inside the furnace tubes, which are assemble in sequenced columns interspersed with burners from the "top fired furnace" type. The columns range from 10 to 14 m in height with 10–20 mm in wall thickness and are formed by welded segments of centrifugally cast heat resistant HP stainless steel tubes modified with niobium and, in some cases, microalloyed with titanium [2–4]. The typical microstructure of the alloy may provide high oxidation resistance and high mechanical performance, especially to creep [5]. The furnace configuration leads to a temperature profile along the columns height, which varies between 600 °C and 1100 °C [2] and causes microstructure modifications with different states of aging [6,7].

Although reformer tubes are designed for a lifespan greater than 100,000 h [1], they might suffer premature damage caused by oxidation, thermal shock, overheating and especially creep [7,8]. Non-destructive magnetic inspection techniques have been developed to be used in the field in order to provide subsidies to estimate the remaining life of the tubes, not only by the detection of voids and cracks but also by the verification of the microstructural aging state of the material [9,10]. It has been observed though, in several occasions, that the magnetic response from the tested tubes has been greater in the surfaces than in the bulk [9,11–13]. It has been found that this augmented response is, in fact, a result of the presence of an oxide scale with magnetic characteristics, formed at high temperature processes.

This work aims to perform a microstructural and magnetic characterization on the external surface of samples, extracted from different column heights, in order to correlate their characteristics to the temperature and the aging state of the material, taking into account the presence of the oxide scale formed under an industrial environment. The external surfaces were characterized by a high-resolution scanning electron microscope (SEM) on backscattering electron mode (BSE) and a chemical composition mapping by X-ray energy dispersive (EDS) was produced. The oxides phases were defined by X-ray diffraction (XRD). A scanning magnetic susceptometer was used to evaluate the magnetic response and correlate it with the aging state of the samples and a magnetic force microscope identified the origin of the magnetism from the external surface.

The present work presents new findings on the morphological and magnetic characteristics of oxide layers formed in HP steels used in steam reforming furnaces. These are important results for non-destructive (ND) integrity assessment inspections and for the remaining life calculation of HP tubes. This effect must be considered when accounting the magnetic response from this tubes in ND tests, preventing therefore, common interpretation errors that can lead to huge economical losses.

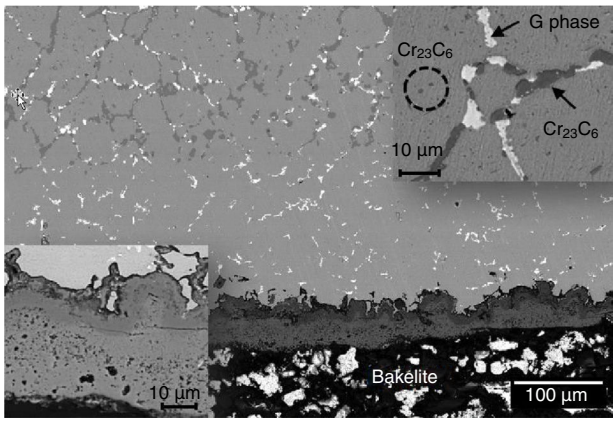

Fig. 1 – Backscattered electron mode image of sample A3, showing the typical morphology of the HP tube external surface.

2. Materials and methods

2.1. *Materials*

Samples were extracted from a tube, that was removed from service after 90,000 h of operation. Tube chemical composition is shown in Table 1. Three samples named A1, A2 and A3 were extracted at different sections (heights) of the tube (1.90 m, 2.70 m and 3.50 m, respectively, in relation to the furnace roof). Different tube sections imply that each sample was exposed to a different operational temperature, result then in different aging states, being classified as states II, IV and V, for the samples A1, A2 and A3, respectively, according Le May et al. [4].

2.2. *Microstructural characterization*

In order to preserve the integrity of the oxide layer, cross-sectional tube sample were cut in a diamond abrasive disc and embedded into a conductive Bakelite resin. The microstructural characterization of the external oxide scale was performed using a high resolution Dual Beam scanning electron microscope, coupled to the energy-dispersive X-ray spectroscope. Morphological characteristics of the external surface were analyzed on the backscattered electron mode. The distribution and composition of the chemical elements on the oxide layer were observed by EDS mapping. The thickness of

Table 1 – Chemical composition of the modified HP alloy analyzed (wt.%).

Tube	Ni	Cr	C	Nb	Si	Mn	W	Ti
A	35.00	25.50	0.54	1.13	1.60	1.30	0.039	0.083

the oxide scale and the chromium carbides depleted zone was measured using an image processing software. The different oxide structures were identified using an X-ray diffractometer, with cobalt radiation (Kα = 1.79 Å). The scanning was performed from 10° to 100° with a scan speed of 0.03°/min.

2.3. *Magnetic characterization*

Magnetic characterization of the external surface was performed on a magnetic force microscope (MFM). MFM analysis was performed on sample A3 at room temperature. The sample was extracted from the tube cross-section and submitted to conventional metallographic preparation without etching. A cobalt-coated silicon probe was used for MFM which exhibits a resonant frequency of 75 kHz. The MFM tip is magnetized using a neodymium magnet (0.46 T of remanent magnetization) prior to the measurements [14]. The first scanning acquired the topography of a scan line on intermittent contact mode. The tip was then lifted to 300 nm from the surface, and the magnetic response of the scan line, caused by the magnetic interaction between the tip and phase, was obtained. External surface magnetic field map was measured by an induced magnetic field, using a scanning DC-susceptometer. Details of the technique are reported elsewhere [9]. The samples were embedded into acrylic resin, with dimensions of 22 × 22 × 1.8 mm. To measure the induced magnetic field Bz, a DC magnetic field of 400 mT was applied and the measurement was made at 150 μm standoff.

3. Results and discussion

3.1. *Oxide scale microstructural characterization*

The external surface of the samples showed a typical morphology as depicted in Fig. 1, presenting only differences on oxide scale and transformed region thickness, as shown

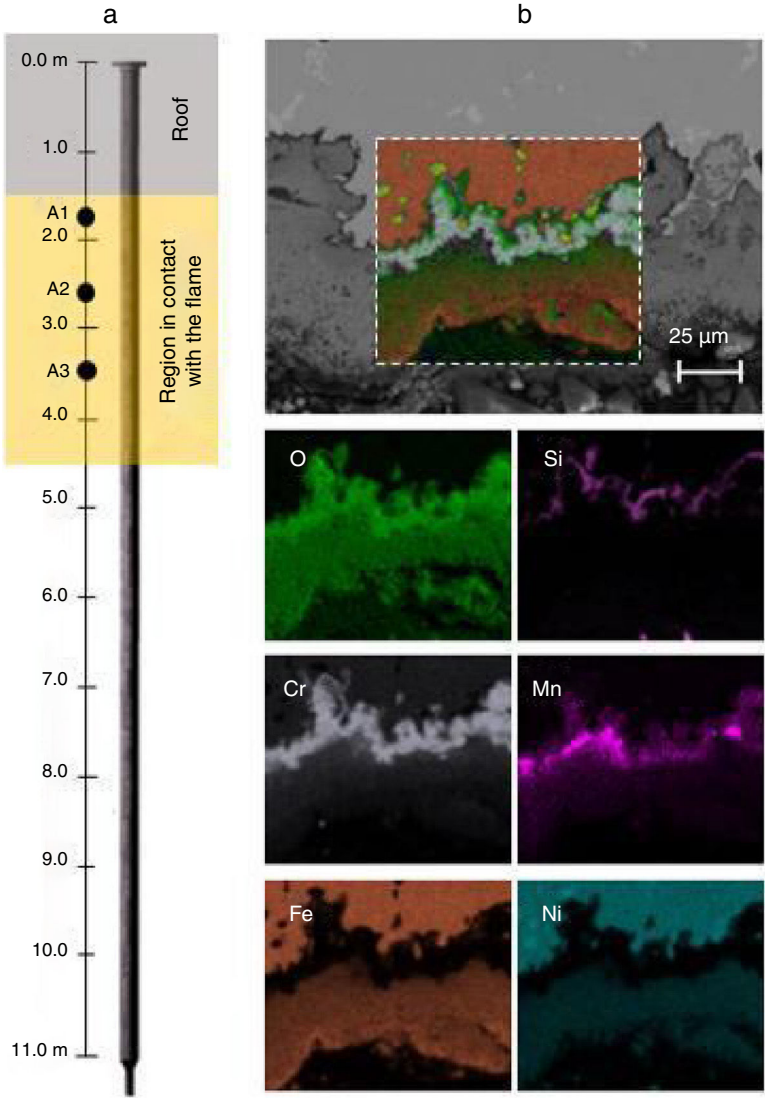

Fig. 2 – (a) Tube scheme showing the position of samples A1, A2 and A3 removed from the reformer column. (b) EDS mapping of sample A2, showing the typical chemical elements present on the oxide scale and their distribution, overlayered at the backscattering image.

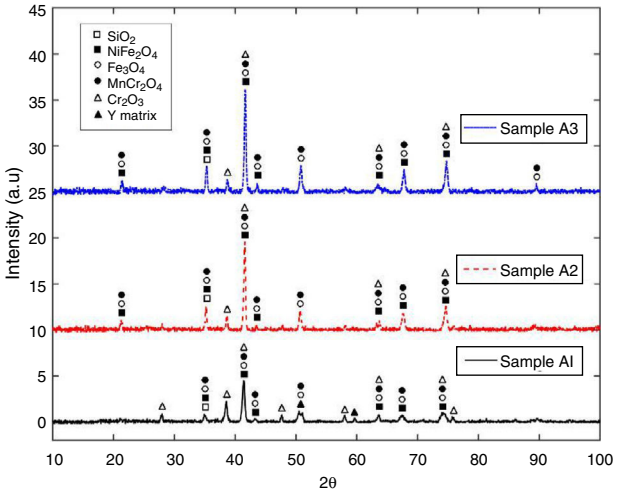

Fig. 3 – X-ray diffraction results, showing the oxides presents in the external oxide scale of the samples A1, A2 and A3.

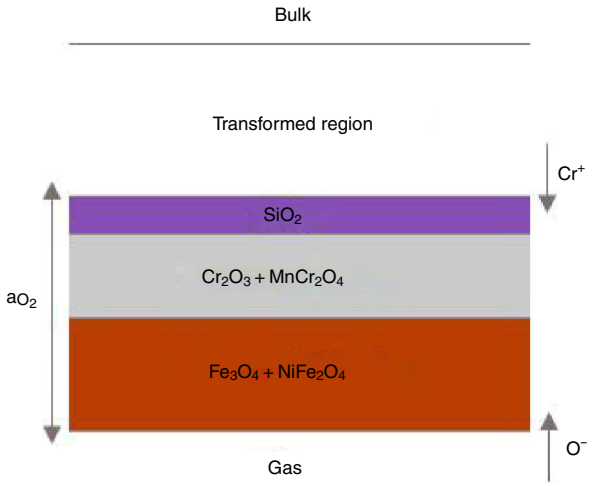

Fig. 4 – Phases distribution model for the external oxide scale formed at modified HP steel tubes used in steam reforming furnaces.

below. Primary and secondary chromium carbides of $M_{23}C_6$ type (dark gray) were observed at the bulk. G phase, usually of composition $Ni_{16}Nb_6Si_7$ (white), was observed in the interdendritic region of the austenitic matrix due to the NbC transformation. The bulk phases were identified elsewhere [5]. A chromium carbides depleted zone was observed in the subsurface of the oxide scale and named "transformed region". A continuous oxide scale with irregular thickness was also observed, with its morphology varying as a function of the temperature. Fig. 2(a) indicates the positions where the samples were extracted from the column. EDS mapping of sample A2, shown in Fig. 2(b), depicts the elements present in the oxide scale. Similar EDS maps were also obtained for samples A1 and A3, that presented the same elemental distribution. A silicon rich layer was well defined at the interface between the oxide and the matrix, followed by an intermediate layer rich in chromium and manganese. The utermost layer of the oxide presents iron and nickel.

Phase identification analysis by XRD for samples A1, A2 and A3 are presented in Fig. 3. In the three analyzed samples, the same phases were identified as SiO_2, $MnCr_2O_4$, Cr_2O_3, $NiFe_2O_4$ and Fe_3O_4. The fundamentals of formation of the oxide scale cannot be discussed, because it is developed at industrial environment. However, XRD and EDS combined analysis indicated that the external surface of the HP tube presented a scale formed of multiple oxide layers, as depicted in the proposed model of Fig. 4. In this model, it can be seen that the scale presents, in fact, a sequence of layers with multiple oxides, followed by the subsurface area free of $M_{23}C_6$ carbides known as "transformed region". Just above, a fine irregular layer of SiO_2 is found, which formation is most likely attributed to the Si affinity to oxygen, that allows this oxide to be formed on a low oxygen partial activity region [15]. A compact layer containing both Cr_2O_3 and $MnCr_2O_4$ was observed after the SiO_2 layer. It was expected that at this point, only a Cr_2O_3 would be present, but due to the high Mn content in the alloy (1.3 wt.%) and its rapid known diffusion through the Cr_2O_3 layer [16], a duplex oxide layer is observed. Finally, in the outermost layer, where the oxygen partial pressure is higher, $NiFe_2O_4$ and Fe_3O_4 spinel are formed.

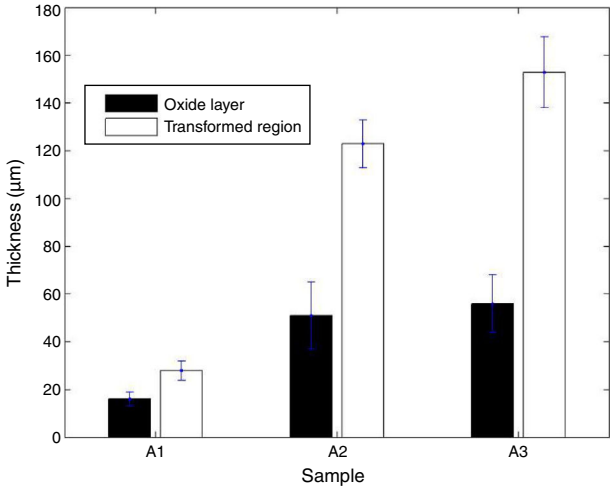

Fig. 5 – Average thickness of oxide layer and transformed region (in μm) for samples A1, A2 and A3.

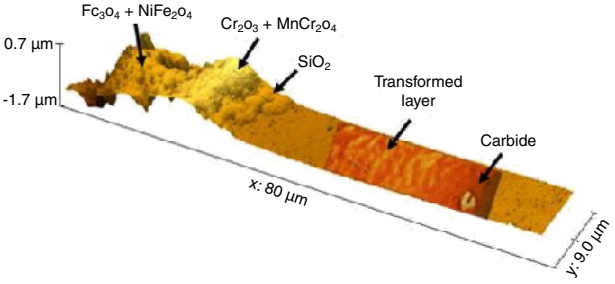

Fig. 6 – Scan line topography, showing the phases presents on it and the ferromagnetic response of the transformed region and the paramagnetic response of the carbide.

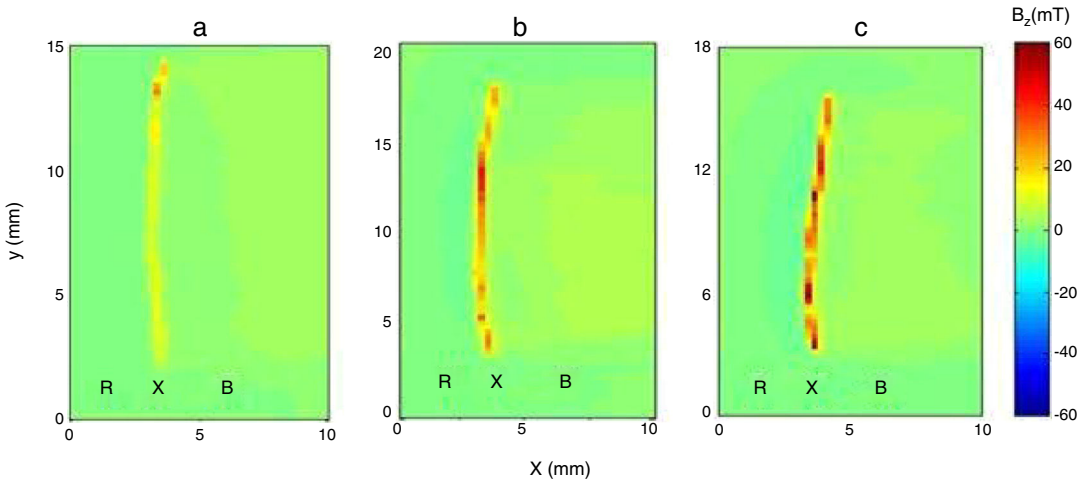

Fig. 7 – Magnetic response of external surface of the three samples under a 400 mT field, applied perpendicularly to the sample surface. Sample with: (a) aging state II – A1, (b) aging state IV – A2 and (c) aging state V – A3. The region (B) represents the bulk of sample, (X) the external surface and (R) the resin in which the samples were embedded.

The average thickness of the oxide layers and the transformed regions of samples A1, A2 and A3 is shown in Fig. 5. Both increase for samples exposed to higher temperatures. Although the transformed region presents a significant increase in its thickness for samples A2 and A3, this effect is not observed for the oxide scales of these samples, as a consequence of partial scale spallation of the outermost layer with Fe_3O_4 and $NiFe_2O_4$ oxides [17]. The steam reforming furnaces undergo temperatures cycling over its operation [2], which leads to cumulative damages in the oxide layers, mainly because of the thermal stresses generated during the cooling. This are the main causes for the occurrence of scales spallation [17]. It was found that the outermost region of the oxide scale, that is rich in Fe and Ni oxides, presented a typical porous appearance. It is known that the porosity of this layer decreases its adhesion to the neighbor oxide layer, reducing its mechanical resistance [18]. This makes the outermost layer of oxide susceptible to spalling resulting from physical and mechanical processes.

3.2. *Magnetic characterization of external surface*

The topography from the region scanned by MFM presented great variations as depicted in Fig. 6. It was possible then to highlight each sublayer of oxide presented with the aid of the EDS mapping results and backscattering electron images. The topography variation influences the MFM results, complicating the identification of magnetic response along the oxide layer [19]. Thus, it was not possible to obtain the magnetic response of the outermost oxide layer containing the Fe_3O_4 and $NiFe_2O_4$ spinel, due to their characteristic porosity. However, it is known that these oxides have a ferromagnetic behavior [20]. The chromium carbides depleted zone presented ferromagnetic behavior when magnetic domains were evidenced. The detected carbide (Fig. 6) showed a paramagnetic response, also observed by [14,21].

The magnetic characterization of the external surface of the reformer tube showed that its magnetic response is due to the transformed layer and the outermost oxide layer consisting of Fe_3O_4 and $NiFe_2O_4$. However, it is not possible to affirm which is predominant. It is important to emphasize that the magnetic response of the external surface of tube is influenced by the integrity of the oxide layer, which is susceptible to partial spallation. Since the oxide scale and the transformed region thickness tend to increase at regions of the tube exposed to higher skin temperatures, it can be concluded that the magnetic response of the external surface also increases with temperature. This fact was verified by scanning the tube cross-section applying a 400 mT field perpendicular to it and measuring the magnetic response in the same direction, Fig. 7. Sample A3 presented a maximum magnetic field response of 50 mT. On other hand, the samples A2 and A1 showed maximum responses of 37 mT and 15 mT, respectively. The bulk of sample presented a response one order of magnitude lower.

4. Conclusions

The proposed characterization for the external surface of samples removed from an Nb–Ti-modified centrifugally cast HP-Type stainless steel tube, that were exposed for 90,000 h to different temperatures inside a reformer furnace, allowed to relate its microstructural characteristics to its magnetic response. The external oxide scale showed a typical distribution sequence of layers that contained a SiO_2 at oxide-matrix interface, followed by $Cr_2O_3 + MnCr_2O_4$, and $NiFe_2O_4 + Fe_3O_4$ at the utermost scale region. Although spallation was observed in many regions along the tube, it was still possible to relate the thickness of both oxide scale and transformed region with the different temperature ranges along the column, i.e. with the different microstructural aging states. The magnetic response of the external surface of the reforming tube originates in the transformed layer where the chromium carbides depletion has occurred and in the utermost oxide region ($NiFe_2O_4 + Fe_3O_4$) which has ferromagnetic characteristics. The ferromagnetism of the external surface,

increases with its thickness, resulting in a stronger magnetic response for tube positions exposed to higher temperatures.

Conflicts of interest

The authors declare no conflicts of interest.

Acknowledgements

The authors would like to thank CAPES, CNPq, Faperj and FINEP for the financial support and Petrobras for supplying the samples for this research.

REFERENCES

[1] Alvino A, Lega D, Giacobbe F, Mazzocchi V, Rinaldi A. Damage characterization in two reformer heater tubes after nearly 10 years of service at different operative and maintenance conditions. Eng Fail Anal 2010;17:1526–41, http://dx.doi.org/10.1016/j.engfailanal.2010.06.003.

[2] da Silveira TL, Le May I. Reformer furnaces: materials, damage, mechanisms, and assessment. Arab J Sci Eng 2006;31:99–119.

[3] Barbabela GD, de Almeida LH, da Silveira TL, Le May I. Role of Nb in modifying the microstructure of heat-resistant cast HP steel. Mater Charact 1991;26:193–7, http://dx.doi.org/10.1016/1044-5803(91)90053-7.

[4] Andrade AR, Bolfarini C, Ferreira LAM, Souza Filho CD, Bonazzi LHC. Titanium micro addition in a centrifugally cast HPNb alloy: high temperature mechanical properties. Mater Sci Eng A 2015;636:48–52, http://dx.doi.org/10.1016/j.msea.2015.03.085.

[5] De Almeida LH, Ribeiro AF, Le May I. Microstructural characterization of modified 25Cr–35Ni centrifugally cast steel furnace tubes. Mater Charact 2002;49:219–29, http://dx.doi.org/10.1016/S1044-5803(03)00013-5.

[6] Le May I, da Silveira TL, Vianna CH. Criteria for the evaluation of damage and remaining life in reformer furnace tubes. Int J Press Vessel Pip 1996;66:233–41, http://dx.doi.org/10.1016/0308-0161(95)00098-4.

[7] Furtado HC, Le May I. High temperature degradation in power plants and refineries. Mater Res 2004;7:103–10, http://dx.doi.org/10.1590/S1516-14392004000100015.

[8] Perez IU, Junior LN, Bueno L, de O, de Almeida LH, da Silveira TF. Short duration overheating in a steam reformer: consequences to the catalyst tubes. Fail Anal Preven 2013;13:779–86, http://dx.doi.org/10.1007/s11668-013-9751-9.

[9] Pereira JMB, Pacheco CJ, Arenas MP, Araujo JFDF, Pereira GR, Bruno AC. Novel scanning dc-susceptometer for characterization of heat-resistant steels with different states of aging. J Magn Magn Mater 2017;442:311–8, http://dx.doi.org/10.1016/j.jmmm.2017.07.004.

[10] Firth DM, Thomas CW, Thakur M, Caporn R. Reformer component management after an overheating incident that resulted in tube failures. In: Conf. 58th AIChE. 2013. p. 187–97.

[11] Stevens KJ, Trompetter WJ. Calibration of eddy current carburization measurements in ethylene production tubes using ion beam analysis. J Phys D Appl Phys 2004;37:501–9, http://dx.doi.org/10.1088/0022-3727/37/3/031.

[12] Hasegawa K, Oikawa T, Kasai N. Development of an eddy current inspection technique with surface magnetization to evaluate the carburization thickness of ethylene pyrolysis furnace tubes. J Nondestruct Eval 2012;31:349–56, http://dx.doi.org/10.1007/s10921-012-0146-8.

[13] Arenas MP, Silveira RM, Pacheco CJ, Bruno AC, Araujo JFDF, Eckstein CB, et al. Magnetic evaluation of the external surface in cast heat-resistant steel tubes with different aging states. J Magn Magn Mater 2018;456:346–52, http://dx.doi.org/10.1016/j.jmmm.2018.02.051.

[14] Arenas MP, Lanzoni EM, Pacheco CJ, Costa CAR, Eckstein CB, De Almeida LH, et al. Separating the influence of electric charges in magnetic force microscopy images of inhomogeneous metal samples. J Magn Magn Mater 2018;446:239–44, http://dx.doi.org/10.1016/j.jmmm.2017.09.041.

[15] Kaya AA, Krauklis P, Young DJ. Microstructure of HK40 alloy after high temperature service in oxidizing/carburizing environment: I. Oxidation phenomena and propagation of a crack. Mater Charact 2002;49:11–21, http://dx.doi.org/10.1016/S1044-5803(02)00249-8.

[16] Xu N, Monceau D, Young D, Furtado J. High temperature corrosion of cast heat resisting steels in $CO + CO_2$ gas mixtures. Corros Sci 2008;50:2398–406, http://dx.doi.org/10.1016/j.corsci.2008.06.001.

[17] Baleix S, Bernhart G, Lours P. Oxidation and oxide spallation of heat resistant cast steels for superplastic forming dies. Mater Sci Eng A 2002;327:155–66, http://dx.doi.org/10.1016/S0921-5093(01)01529-5.

[18] Young DJ. High temperature oxidation and corrosion of metals, vol. 1, first ed. Cambridge, UK: Elsevier Corrosion Series; 2008, http://dx.doi.org/10.1017/CBO9781107415324.004.

[19] Saint-Jean M, Hudlet S, Guthmann C, Berger J. Van der Waals and capacitive forces in atomic force microscopes. J Appl Phys 1999;86:5245.

[20] Marinca TF, Chicinaş I, Isnard O, Pop V, Popa F. Synthesis, structural and magnetic characterization of nanocrystalline nickel ferrite – $NiFe_2O_4$ obtained by reactive milling. J Alloys Compd 2011;509:7931–6, http://dx.doi.org/10.1016/j.jallcom.2011.05.040.

[21] Silva IC, Rebello JMA, Bruno AC, Jacques PJ, Nysten B, Dille J. Structural and magnetic characterization of a carburized cast austenitic steel. Scr Mater 2008;59:1010–3, http://dx.doi.org/10.1016/j.scriptamat.2008.07.015.